BJET
(Bayero Journal of Engineering and Technology)
https://bjet.ng/index.php/jet

Research Article
2026, Vol. 21 (1), 55-64

DEVELOPMENT OF FLC-BASED ANTILOCK BRAKING SYSTEM WHEEL SLIP CONTROL FOR HALF AND QUARTER VEHICLE MODELS

Y. A. Muhammad[1] and H. A. Bashir[2]

[1]Department of Mechatronics Engineering, Federal University Dutsin-Ma, Katsina-Nigeria
[2]Department of Electrical Engineering, Bayero University, Kano-Nigeria

[*]Corresponding author: yahaya160@gmail.com

Received: 09-10-2025
Revised: 24-12-2025
Accepted: 06-01-2026
Published: 11-01-2026

Abstract *An antilock braking system (ABS) is an essential mechanism that improves the braking system of a vehicle. Different methods were used to design a better controller in order to improve the system. Literature studies had shown that the major technique used in modelling the system is the quarter-vehicle model for uncomplicatedness in the controller design. A half-vehicle model was adapted and will have more dynamic parameters of the overall system as compared to the quarter-vehicle model. In this work a fuzzy logic controller (FLC) for each wheel is designed separately; this is because the frictional force for the front wheel is higher than that of the rear wheel. Using the same vehicle parameters for the half model, another FLC is designed for the quarter model. The performance of the two models was evaluated by comparing the stopping distance of the two models. Simulation results show that the FLC-controlled half-vehicle model performed better than the quarter-vehicle model in terms of stopping distance, which is the critical factor in ABS. Using the same vehicle parameters for both models, simulation results have shown that the percentage reduction in terms of stopping distance has improved by 16.3% for the FLC-controlled half-vehicle model as against that of the FLC-controlled quarter-vehicle model, as well as a 13.8% improvement with the proposed FLC as against the sliding mode controller with disturbance observer. Evaluation results show that the stopping distance of a vehicle with ABS is better with the half-vehicle model and FLC than with the commonly used quarter-vehicle model; this improves safety and can save more lives, as the vehicle has more tendency to stop as compared with the quarter-model design.*

Key words: Fuzzy Logic Controller; Antilock Braking System; Quarter-Vehicle; Half-Vehicle; Stopping Distance

1. Introduction

ABS is regarded as an essential component of road safety because it keeps the car stable and steerable during heavy braking by preventing the wheels from locking (Abd El-Fatah, *et al.*, 2021). Whenever vehicle wheels lock while braking, the vehicle loses its ability to maneuver laterally, which makes it unsteerable and greatly increases the likelihood of an accident (Amirkhan & Molaie, 2022). The ABS's major job is to keep the wheels from slipping too much or too little, which allows the car to slow down with maximum braking while still being steerable (Han, *et al.*, 2019). Mathematically, the ABS can be characterized as a model that needs to be constructed and tested. A collection of subsystems makes up the ABS system, which collectively lowers a car's speed until it stops (Algadah & Alaboodi, 2019). Wheel slip can result in a vehicle crash by extending the stopping distance of a braking vehicle and, in certain cases, losing steering stability (Agwah & Eze, 2022).

Globally, the number of automobiles is always growing; over 80 million cars were sold worldwide in 2021, representing a 4.96% rise over the previous year. Unquestionably, vehicles are now considered essential in people's daily lives (Wang, *et al.*, 2022). Active vehicle safety systems (AVSSs) are essential for drivers because of the growing number of road vehicles and improvements in their design that allow them to operate at faster speeds. Across the globe, one of the biggest concerns is road vehicle fatalities (Challa, *et al.*, 2020). According to statistics on contemporary auto accidents, the ABS malfunctions are to blame for over 20% of them (Fu, 2022).

The design of the ABS is one of the trickiest aspects of wheel slip control (WSC). Wheel dynamics are managed by ABS, an active safety device, when hard braking occurs. The system's goal is to maximize braking efficiency without sacrificing steering and stability (Pretagostini, *et al.*, 2020). Uncertainties, measurement noise, parameter changes, and nonlinearities all contribute to the complexity of ABS design. Due to the fact that the road and vehicle conditions are complex, the braking process of the ABS is characterized by nonlinearity, time variation, and uncertainty (Pretagostini, *et al.*, 2020).

Recently, various control strategies were proposed for ABS, including PID control, intelligent control, and robust control. These approaches attempt to precisely manage the slip ratio in order to maximize the effectiveness of tire force in the longitudinal direction (Wang, *et al.*, 2021). This is mostly because PID controllers are easy to build and use, have a simple structure that engineers can quickly understand, and have strong performance to handle the global changes in industrial processes (Ahmad, *et al.*, 2018). A reliable nonlinear controller design for wheel speed tracking was developed in (Gampa, *et al.*, 2023), the authors developed a fuzzy logic-based ABS by considering a quarter-vehicle model. Two FCL controllers were devised: one to manage the braking torque using projected slip, and the other to estimate the road condition (Gampa, *et al.*, 2023). Elsewhere, an ABS robust control was developed based on road surface identification to increase the system's robustness. The technique determines the ideal dynamic slip rate, evaluates the road adhesion coefficient in real time, and identifies roads using a fuzzy logic control algorithm (Qi, *et al.*, 2022). Similarly, different non-linear controllers were primarily used to represent the ABS controller, and the results were compared with the suggested algorithm's performance with an existing method in terms of vehicle stopping distance and stopping time (Dankan, *et al.*, 2019).

An investigation of the performance of ABS in relation to weight change, road friction coefficient, and road incline was conducted in (Rajguru, *et al.*, 2014). The authors developed a fuzzy-GA-tuned PID controller to address the ABS challenges. In addition to preserving the intended range of tire slip rate, the control system tends to shorten stopping distances (Rajguru, *et al.*, 2014). Similar to this, ABS relied on sliding mode control as its primary control algorithm because of its resilience; yet, its performance was significantly impacted by chattering, which was impossible to eradicate. A road surface recognition-based ABS sliding mode variable structure control method was presented to improve performance and get rid of chattering (Qi, *et al.*, 2022).

Generally, the use of the quarter-vehicle model in wheel slip control gives rise to long stopping distance; this is because in the quarter-vehicle model system, the vehicle mass is constant and mass transfer during braking is ignored. However, the vehicle's engine and gearbox weight act majorly on the front side; therefore, the vehicle's wheels may be on different traction surfaces at any given time, and the normal force on the front wheels will be greater than that on the rear wheels. Hence, the front and rear wheels tend to experience varying frictional forces at any given time. This paper aims to investigate the impact of wheel slip control technique on a half-vehicle model. As a simulation-based study, this work employs a half-vehicle model to regulate nonlinear wheel slip and improve overall vehicle safety and maneuverability by cutting down on stopping distance.

2. Background on ABS System

One of the safety features that is frequently present in contemporary cars is the ABS. In order to keep steering control and minimize slippage, it is made to keep the wheels from locking up when braking (Dankan, *et al.*, 2019). The parts of the ABS are as follows:

2.1 Pedal

One part of the car's antilock braking system that the driver can use to start the braking process is the brake pedal. It is situated on the driver's-side floorboard. The car slows down or stops when the driver applies pressure to the brake pipes through the pedal with his foot, activating the braking system. The movement of the brake pads and shoe creates a high brake pedal, as shown in Figure 1 (AGCO, n.d.).

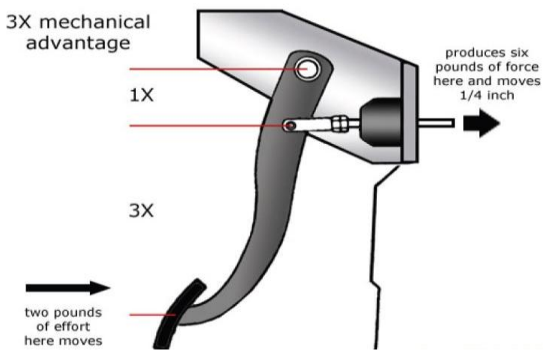

Figure 1: Brake Pedal Schematic Diagram (AGCO, n.d)

2.2 Master Cylinder

The quality of the braking system's processing and operation determines how well the master cylinder is, which is the most important component in the vehicle braking system (Zhao, *et al*., 2021).

A master cylinder transfers a liquid through a system using hydraulic pressure. Generally, there are three primary parts to a braking system. These are the master cylinder and braking pedal, as well as the wheel braking mechanism (Saibabu & Prakash, 2018). Figure 2 displays the diagram of the entire master cylinder (Kamsi Parts, 2020), when the pedal is pressed, the master cylinder supplies brake fluid to the ABS and subsequently to the wheels. The fluid presses the brake shoes, or pads, at the wheels up against revolving disks or drums (Saibabu & Prakash, 2018). The brake fluid is kept in a reservoir attached to the master cylinder, which, in a hydraulic braking system, starts and controls braking action with a simple piston (Saibabu & Prakash, 2018).

Figure 2: *Hydraulic Master Cylinder (Kamsi Parts, 2020)*

2.3 ABS and ABS Sensors

This module is the computer that assists in braking; it is the brain of the ABS system. To find out if any wheels are going to lock up, it takes data from the speed sensors and processes it. It communicates with the hydraulic modulator by signals based on the information it has received. A vehicle wheel may accelerate when the pressure is released as it approaches lock-up. If a wheel is going too fast, you can slow it down by exerting greater pressure. The brake control module may choose to operate in a pressure hold mode when the two wheels are moving at almost the same speed (ABS, 2011). The module's figure is displayed in Figure 3 (PÁGINA, 2019). Consequently, the ABS optimizes the amount of friction between the tires and the pavement when it is activated.

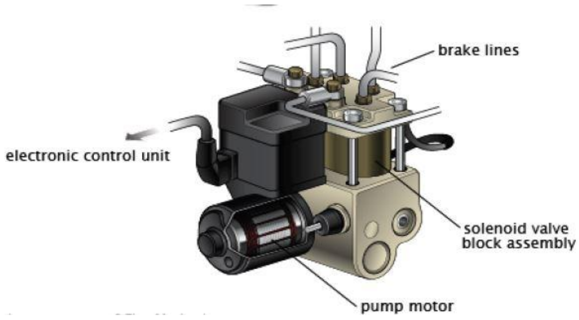

Figure 3: *ABS Control Module (PÁGINA, 2019)*

Sensors

These sensors are found at the wheels or occasionally inside the gearbox. As seen in Figure 4 (PÁGINA, 2019), they track the speed at which each wheel rotates and give the ABS control module data in real time. These sensors monitor each wheel's spin continually to decide if the ABS system should take over the driver's manual brakes in slick circumstances. The speed sensor measures rotations and evaluates wheel continuity. ABS can kick in to control braking when it detects rotational changes (ABS, 2011).

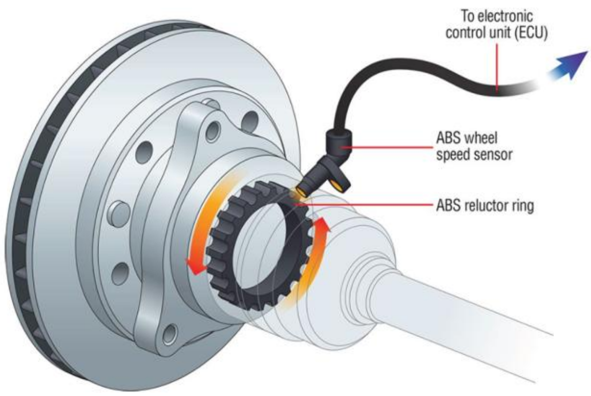

Figure 4: *Wheel Speed Sensor Configuration (PÁGINA, 2019)*

3. Methodology

3.1 Vehicle Model

3.1.1 Half Vehicle Model

A longitudinal model of a vehicle, as shown in Figure 5, is considered whereby each wheel remains on the same road surface and assumes the lateral tire forces, the yaw moment, aerodynamic drag forces, and roll resistance to be zero during a braking maneuver. Also, the link between the vehicle mass and the ground (i.e., through the vehicle suspension, wheel, and tire) is assumed to be rigid in the longitudinal direction. Based on the above assumptions and the simplified longitudinal model of a vehicle, it can be deduced that a weight transfer takes place about the center of gravity due to longitudinal deceleration.

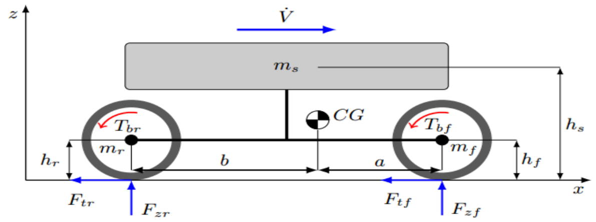

Figure 5: Free body diagram of a Vehicle (Phadke, et al., 2019)

The symbols used in Figure 5 are defined in Table 1.

Table 1: List of parameters (Phadke, et al., 2019)

Parameter	Description	Value
a	Distance of front axle from CG	$1.11m$
b	Distance of rear axle from CG	$1.67m$
g	Acceleration due to gravity	$9.81ms^{-1}$
h_f	Height of front unsprung mass	$0.34m$
h_r	Height of rear unsprung mass	$0.325m$
h_s	Height of sprung mass	$0.542m$
I_f	Moment of inertia of front wheel	$0.9kg.m^2$
I_r	Moment of inertia of rear wheel	$0.9kg.m^2$
m_f	Front unsprung mass	$80kg$
m_r	Rear unsprung mass	$80kg$
m_s	Sprung mass of the vehicle	$1370kg$
m_t	Total mass of the vehicle	$1530kg$
R_w	Radius of the wheel	$0.325m$

The deceleration of the vehicle is given by

$$\dot{V} = \ddot{x} = -g\left[\frac{\mu(\lambda_f)m_1 + \mu(\lambda_r)m_2}{m_t - \mu(\lambda_f)m_3 + \mu(\lambda_r)m_3}\right]. \quad (1)$$

And the wheels angular velocity for the front and rear wheels are as follows:

$$\dot{\omega}_f = \frac{1}{J_f}[\mu(\lambda_f)(m_1 g - m_3\ddot{x})R_w - T_{bf}] \quad (2)$$

$$\dot{\omega}_r = \frac{1}{J_r}[\mu(\lambda_r)(m_2 g + m_3\ddot{x})R_w - T_{br}] \quad (3)$$

3.1.2 Quarter Vehicle Model

For simplicity, the quarter car model was used, and it is thought that the vehicle system adheres to stiff body dynamics (Amirkhan & Molaie, 2022). A set of parameter definitions is given in Table 1, and the dynamics analysis of vehicle longitudinal motion is based on the one-wheel vehicle model, which is depicted in Figure 6 (Gampa, *et al.*, 2023). The quarter-vehicle model, which is one of the most widely used models in the literature, is thus presented in this section. Figure 5 shows the forces applied to an automobile tire during braking. The quarter-vehicle model's equations are as follows (Gampa, *et al.*, 2023): The vehicle's velocity tends to zero when the brake is applied, then the velocity changes negatively, resulting in a deceleration.

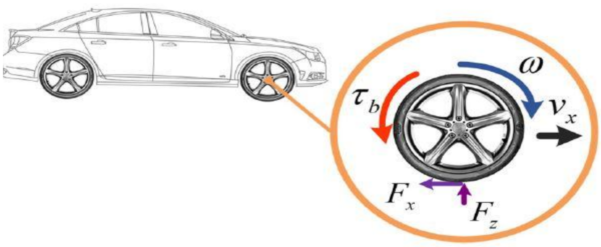

Figure 6: The Forces Applied to a Car Wheel During Braking (Amirkhan & Molaie, 2022)

From Newton's second law of motion

$$m\frac{dV_x}{dt} = -F_x\,, \quad (4)$$

Taking the algebraic sum of the torque in wheel of Figure 6, we have equation (5)

$$J\frac{d\omega_x}{dt} = F_x R_w - T_b, \quad (5)$$

Where

$$F_x = \mu(\lambda)mg, \quad (6)$$

$$V_x = \omega_x R_w. \quad (7)$$

3.1.3 Road -Tire Model

Tire behavior models, which explain how tires interact with the road, are commonly used to determine tire forces. The goals of the system analysis are what dictate which of these models to select and how difficult the decision will be. For example, the Fiala and Dugoff models are commonly employed for

BJET, 2026, Vol. 21(1), 55-64

detection because of their great precision (Amirkhan & Molaie, 2022). However, other very precise models, such as the Magic Formula, are less frequently used because of their dependence on a large number of variables and factors. The Burckhardt model, the Magic Formula, and the Dugoff model are three of the more popular and frequently applied models in this area (Amirkhan & Molaie, 2022). Burckhardt model. The Burckhardt model is frequently employed to simulate nonlinear tire-road relationships. Among the factors influencing the coefficient of friction between the wheel and the road are wheel slip, temperature, humidity, and vehicle speed. The wheel's slippage can be represented by an empirical function (Unguritu & Nichitelea, 2023). The Burckhardt model can be used to determine the friction coefficient for a specific standard road surface, as shown in equation (5) (Abdulkareem, *et al.*, 2022).

$$\mu(\lambda) = c_1\left(1 - e^{-c_2\lambda}\right) - c_3\lambda \qquad (8)$$

The coefficient values for the various road surfaces are shown in Table 2.

Table 2: *Parameters of Various Standard Road Surfaces (Abdulkareem, et al., 2022)*

Road surfaces	c_1	c_2	c_3
Dry asphalt	1.28	23.99	0.52
Wet asphalt	0.85	33.82	0.35
Dry concrete	0.40	33.71	0.12

3.2 Proposed Fuzzy Logic Controller Design

To maintain the wheel slip ratio within a predetermined range, the ABS control operation is necessary. ABS's closed-loop control method uses wheel slip feedback to compare to the fixed point of 0.2, which is later varied from 0.2 to 0.1 (Unguritu & Nichitelea, 2023). Figure 7 depicts the proposed ABS controller.

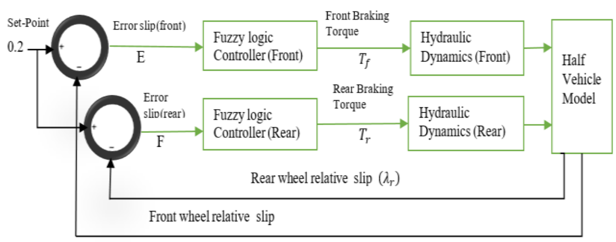

Figure 7: *Proposed ABS Controller Model*

3.2.1 Fuzzy Inference System

There are basically two prominent fuzzy inference engines, Mamdani and Takagi-Sugeno (T-S), which are used in the design of fuzzy logic controllers. In this design two controllers are required to be designed, making the rules interpretable and enabling the controller to handle the non-linear relationship easily. The Mamdani approach is used. It also gives more qualitative results as compared to T-S.

3.2.2 Input and Output Parameters

As shown in Figure 7, two parameters are considered: the error signal (wheel slip), which serves as the input to the controllers, and the second parameter, which is the braking torque (Nm), which defines the output of the controllers. Due to the dynamics of the system, the two controllers are interrelated even though they have isolated inputs and outputs. The magnitudes of these parameters varied at any instant of time.

3.2.3 Universe of Discourse

In order to determine the input and output range of the controllers (universe of discourse), two PID controllers were implemented in the vehicle dynamic model using the Simulink toolbox of MATLAB and tuned to obtain some reasonable responses by minimizing time domain specification (overshoot, rise time, and steady-state error). This was achieved by the use of the PID control tuner toolbox in MATLAB. The inputs and outputs of the PID controllers were measured and taken to the workspace. From the plots of both the input and the outputs, the input and output ranges are roughly obtained. The input range for the front wheel controller (E) is $[-0.5\ to\ 0.5]$ and the corresponding output range (T_f) is $[-1000\ to\ 1000]$. Similarly, the input range for the rear wheel controller *(F)* is $[-0.4\ to\ 0.4]$ and the corresponding output range (T_r) is $[-700\ to\ 700]$. These values were used to initialize the FCL controllers.

3.2.4 Linguistic states and Membership Function

After identifying the relevant input and output variables and their ranges, a meaningful state called the linguistic state for each variable is defined. The following linguistic states for the front wheel controller are considered: Error *(E)* for the front wheel is represented using three linguistic states. This is because the design required two FLCs, and the controllers are dynamically correlated. Also, the input and output ranges can be covered with the three linguistic states.

E_1 : Small slip
E_2 : Medium slip
E_3 : Large slip

The corresponding output, braking torque (T_f) is represented using three linguistic states as well.

P_1 : High torque
P_2 : Medium torque
P_3 : Low torque

Similarly, for the rear wheel, the following linguistic states for the front wheel controller are considered:
Error *(F)* for the front wheel is represented using three linguistic states.
F_1 : Small slip
F_2 : Medium slip
F_3 : Large slip
The corresponding output, braking torque (T_r), is represented using the following linguistic states.
M_1 : High torque
M_2 : Medium torque
M_3 : Low torque
Triangular membership functions were used in this design due to their lesser computational complexity and ability to accommodate a wide range of fuzzy sets. They also provide smooth transitions across membership values, which ease the defuzzification process. Figures 8 and 9 show the configuration of the membership functions for the two controllers for the front and rear wheels, respectively.

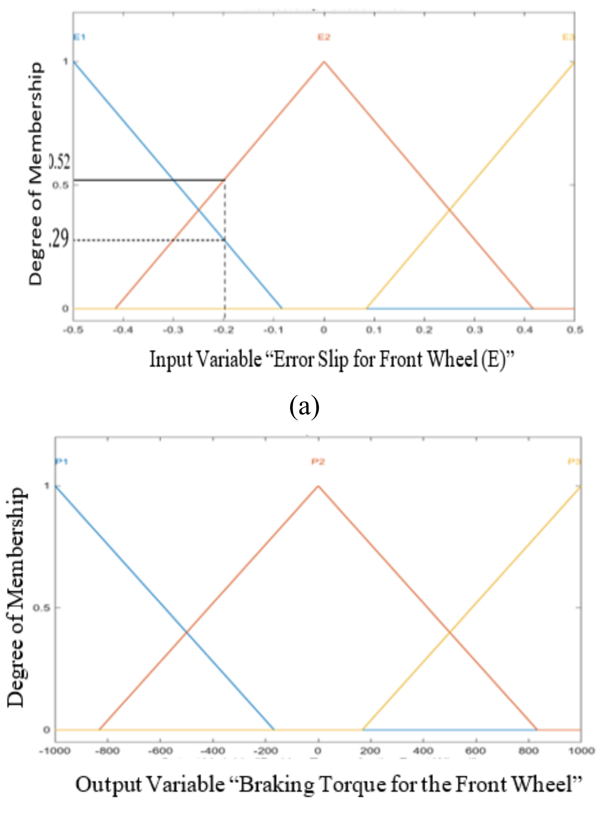

***Figure 8**: Membership Function for the Front Wheel: (a) Input (b) Output*

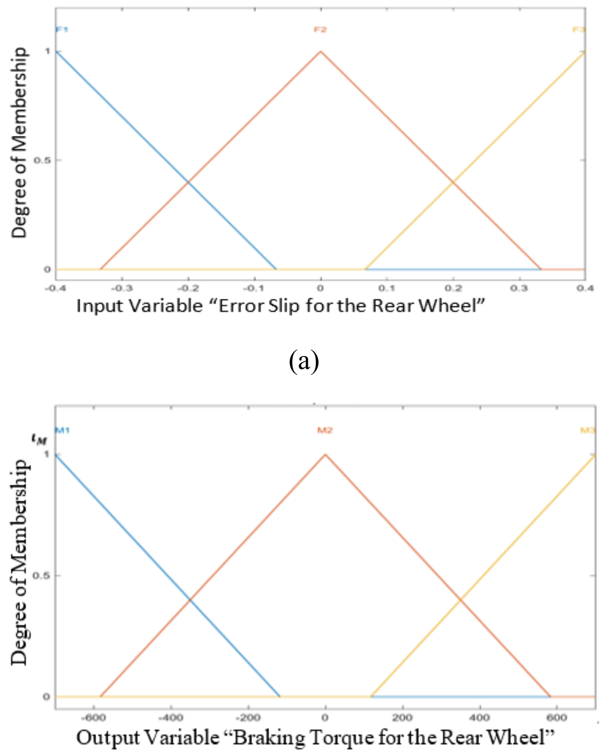

***Figure 9:** Membership Function for the Rear Wheel: (a) Input (b) Output*

The following rules were used to initialize the front wheel controller.
Rule 1: If the input is small slip (E_1), then the output is high torque (P_1).
Rule 2: If the input is medium slip (E_2), then the output is medium torque (P_2).
Rule 3: If the input is large slip (E_3), then the output is low torque (P_3).
Similarly, for the rear wheel
Rule 1: If the input is small slip (F_1), then the output is high torque (M_1).
Rule 2: If the input is medium slip (F_2), then the output is medium torque (M_2).
Rule 3: If the input is large slip (F_3), then the output is low torque (M_3).
After the design, various defuzzification methods were evaluated analytically, and the centroid method gives the best results. All the above-designed parameters were used to initialize the controllers; thereafter, the controllers were tuned to obtain the desired results. Various toolboxes in MATLAB (2023b), such as the control toolbox, Simulink, the FLC toolbox, and the System Identification toolbox, were used in this design.

4. Simulation Results and Discussion

4.1 Evaluation of wheel Slip Variation

After the controllers' design, various slip ratios were analysed at different speeds in order to determine the best wheel slip for the system. As it was stated in the introduction, the wheel slip that corresponds to the maximum coefficient of friction is between 0.12 and 0.22. Slips of 0.1, 0.15, and 0.2 at different speeds were analysed. In the first instant a slip of 0.2 was used, and the speed was varied from $80ms^{-1}$, $60ms^{-1}$ and, $40ms^{-1}$. Figure 9 shows half vehicle model wheel slip for the front and rear wheels with a dash line. The ABS is activated at the start of the simulation. The desired wheel slip is indicated in Figure 10 (a) and (b) with a dashed line. The ABS is activated at the start of the simulation.

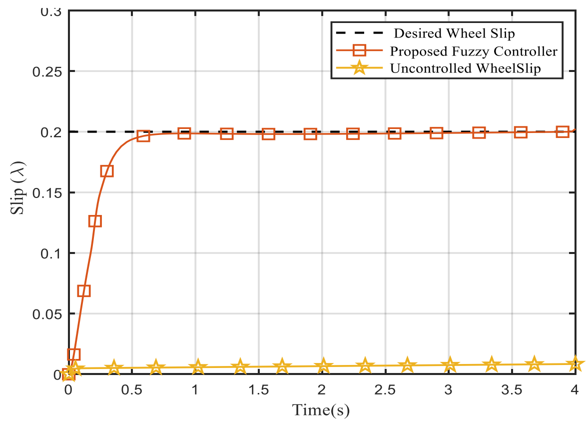

(a)

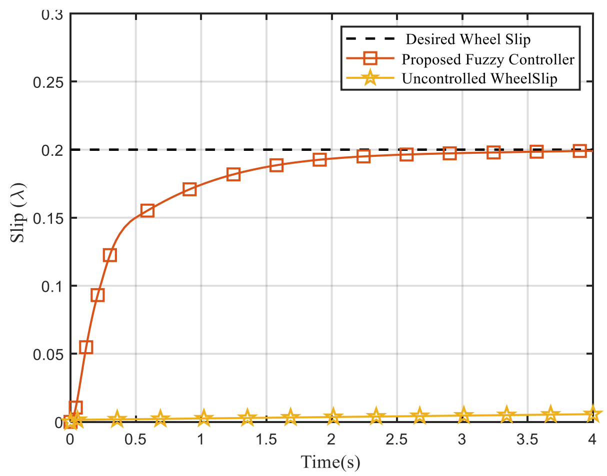

(b)

Figure 10: Slip Behaviour for Half Vehicle Model at Slip of 0.2; (a) Front Wheel (b) Rear Wheel

It can be seen that the control action for the rear wheel is not as fast as that of the front wheel, which is as a result of mass transfer during braking from the rear wheel to the front wheel. This adds more weight to the front wheel and makes the controller in the rear wheel not as fast as that of the front wheel.

The reference wheel slip was changed to 0.15, as shown in Figure 11, which shows similar results as compared to the results obtained with a reference wheel slip of 0.2.

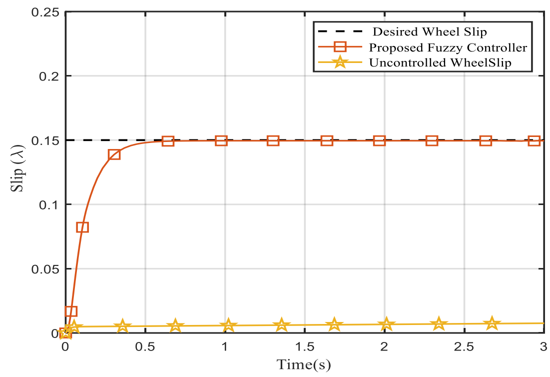

(a)

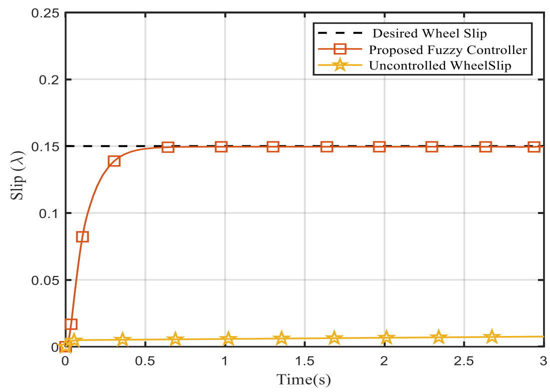

(b)

Figure 11: Slip Behaviour for Half Vehicle Model at Slip of 0.15; (a) Front Wheel (b) Rear Wheel

At this reference slip, the speed was varied from high to medium to low. This reference slip has a better response as compared to the reference of 0.2.

Finally, a wheel slip of 0.1 is used as a reference. After the controller was tuned, the wheel slips and the corresponding reference slips are shown in Figure 12.

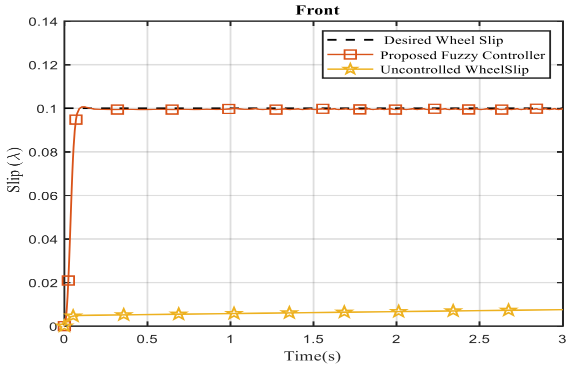

(a)

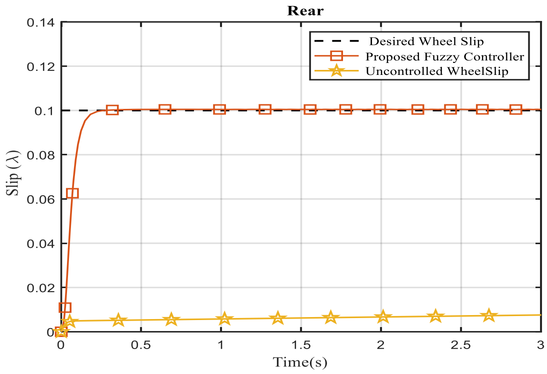

(b)

Figure 12: Slip behaviour for Half Vehicle Model at Slip of 0.10; (a) Front Wheel (b) Rear Wheel

4.2 Evaluation of the Stopping Distance

The stopping distances were evaluated at different speeds and at the wheel slip references of 0.2, 0.15, and 0.1. At the wheel slip of 0.2 and 0.15, the stopping distance is almost the same, as there is not much variation in the stopping distance, as shown in Figure 13.

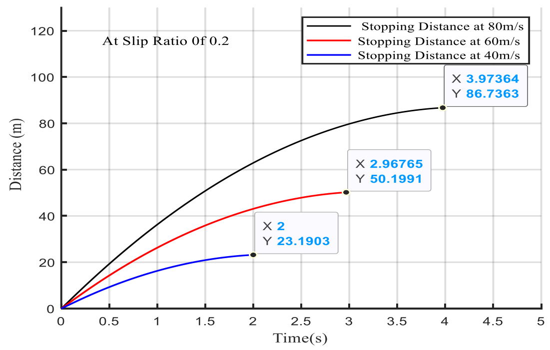

(a)

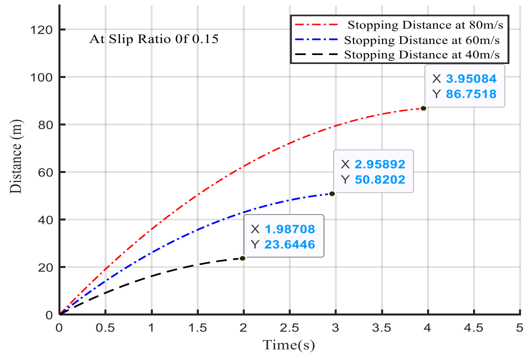

(b)

Figure 13: Stopping Distance for the Half Vehicle Model: (a) Slip of 0.2 (b) Slip 0.15

Then, at the slip of 0.1, the stopping distance increased at both high and low speeds as compared to the stopping distance when the wheel slip was 0.2 and 0.15, as shown in Figure 14(a).

The stopping distances for the three cases of wheel slip of 0.1, 0.15, and 0.2 at medium speeds were compared. This shows that the wheel slip of 0.1 is having a high stopping distance at various speeds. The stopping distances for the wheel slip of 0.2 and 0.15 are almost the same, as shown in Figure 14(b).

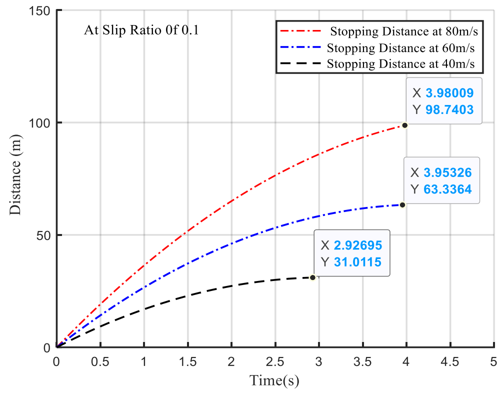

(a)

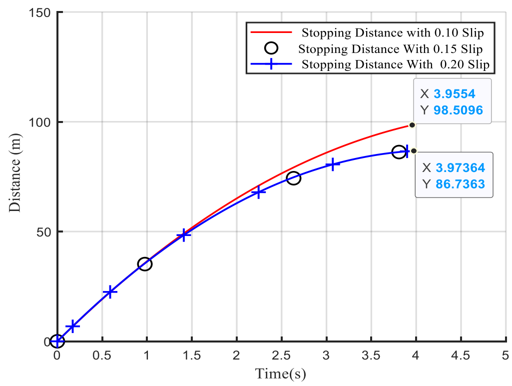

(b)

Figure 14: Stopping Distances for the Half Vehicle Model at: (a) Slip of 0.1(b) Slips of 0.1, 0.15 and 0.2

4.3 Performance Comparison for the Stopping Distance of Half versus Quarter Vehicle models

The same parameters used for the half-vehicle model are used for the quarter-vehicle model, which gives the plot of distance in meters versus time. In order to show the results obtained from the two vehicle models, we compared the simulation results. The comparison was done in terms of stopping distance, which is shown graphically. Figure 15 gives the simulation results of the comparison between the two models.

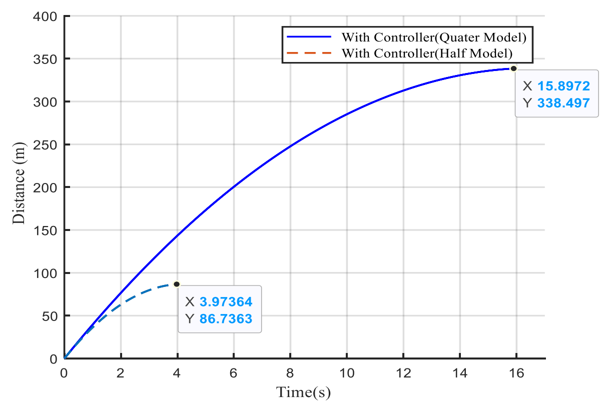

Figure 15: *Stopping Distance for Quarter vs. Half-Vehicle Models*

The stopping distance and time for the quarter-vehicle model are longer than those of the half-vehicle model (see Table 3). This is because the quarter model does not fully describe the braking dynamic model. The effect of mass transfer during braking from the front wheel to the rear wheel cannot be accounted for in the quarter model, nor can the dynamic changes of the center of gravity of the vehicle during braking.

Table 3: *Comparison of Simulation Results* $(80\, m/s)$

	Stopping distance (m)		Stopping time (sec)	
	Without controller	With controller	Without controller	With controller
Half VM	751.8	86.7	30.0	4.0
Quarter VM	1216.5	337.7	44.9	15.5

Percentage reduction in stopping distance from each model is given by (8).

$$\%\, reduction = \left(1 - \frac{Controlled\ Stopping\ Distance\ (m)}{Uncontrolled\ Stopping\ Distance\ (m)}\right) \times 100\% \quad (8)$$

Half VM:

$$\%\, reduction = \left(1 - \frac{86.7}{751.8}\right) \times 100\% = \mathbf{88.5\%}$$

Quarter VM:

$$\%\, reduction = \left(1 - \frac{337.7}{1216.5}\right) \times 100\% = \mathbf{72.2\%}$$

$$\%\ \text{Improvement} = 88.5\% - 72.2\% = \mathbf{16.3\%}$$

4.4 Comparison of the proposed FLC-based with a Sliding Mode Controller

The stopping distance obtained from the model with the sliding mode controller (Phadke, Shendge, & Wanaskar, 2020) is compared against the one obtained from the proposed fuzzy logic controller. This was done with the same half-vehicle model and at the same initial velocity. The comparison of the two controllers is shown in Figure 16.

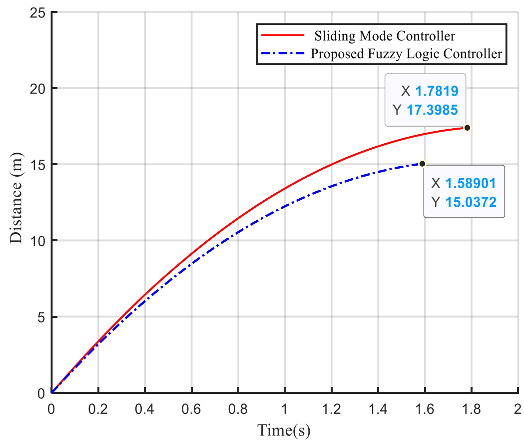

Figure 16: *Stopping Distance for the both Controllers*

From Figure 16, it can be seen that the stopping distance with the sliding mode controller is 17.4 m and that of the proposed FLC is 15 m, which gives a difference of 2.4 m. This could be due to the fact that the internal structure of the FLC was able to match the nonlinearity of the ABS system better than the SMC controller. The SMC is generally known to suffer from inherent chattering problem. The percentage improvement between the two controllers is 13.8% as evaluated in the following equation (9).

$$\% \, Improvement = \left(\frac{Stopping\ Distance\ (m)(SMC-FLC)}{Stopping\ Distance\ (m)\ with\ SMC}\right) \times 100\% \quad (9)$$

$$\% \, Improvement = \left(\frac{17.4 - 15}{17.4}\right) \times 100\% = \mathbf{13.8}\%$$

5. Conclusion

Designing a better control for ABS is difficult as a result of nonlinearity and uncertainty in the system, which often results in long stopping distances during braking. Fuzzy logic controllers were designed on both the half and quarter vehicle models. The results of various sections of the simulation are presented. The effect of a fuzzy logic controller on wheel slip with respect to the stopping distance as a critical parameter is analyzed. As key contributions, the effect of mass transfer during braking as well as the sprung and unsprung masses is shown by comparing the results of the half and the quarter vehicle models. This is seen both graphically and numerically: the half-vehicle model is better than the quarter-vehicle model in terms of wheel slip control, and the FLC-controlled ABS has improved stopping distances of about 16.3% as compared to the quarter-vehicle model. In comparison with the sliding mode controller with disturbance observer, the FLC on the half-vehicle model achieved an 88.5% reduction in stopping distance and performed 13.8% better than an SMC controller in terms of stopping distance.

References

Abd El-Fatah, S. A., Sharkawy, A.-N., Moaaz, A. O. & Ghazaly, N. M., 2021. A Comparative Study of Different Control Methods for Anti-Lock Braking System (ABS). *SVU-International Journal of Engineering Sciences and Applications*, 11 June, Volume 2, pp. 27-34.

Abdulkareem, A. Q., Humod, A. T. & Ahmed, O. A., 2022. A Data Based Method Road Surface Parameters Estimation for Anti-Lock Braking System. *Diyala Journal of Engineering Sciences,* Volume 15, pp. 130-141.

ABS, 2011. Mechanical World. [Online] Available at: http://mechlover.blogspot.com [Accessed 12 December 2023].

AGCO, 2023. AGCO Automotive Corporation. [Online] Available at: https://www.agcoauto.com /content/news/p2_articleid/265 [Accessed 27 November 2023].

Agwah, B. C. & Eze, P. C., 2022. An Intelligent Controller Augmented with Variable Zero Lag Compensation for Antilock Braking System. *International Journal of Mechanical and Mechatronics Engineering,* Volume 16, pp. 303-310.

Ahmad, F. et al., 2018. Fuzzy Fractional PID Gain Controller for Antilock Braking System using an electronic wedge Brake Mechanism. *Int. J. Vehicle Safety,* 10(2), pp. 97-121.

Algadah, K. M. & Alaboodi, A. S., 2019. Anti-Lock Braking System Components Modelling. *International Journal of Innovative Technology and Exploring Engineering,* December, 9(2), pp. 3969-3975.

Amirkhan, A. & Molaie, M., 2022. Fuzzy Controllers of Antilock Braking System: A Review. *International Journal of Fuzzy Systems*, 18 October. pp. 1-23.

Challa, A. et al., 2020. Antilock Braking Control Algorithms Antilock Braking Control Algorithms. Chennai, India, *Elsevier.*

Dankan, G. V. et al., 2019. Modelling and Performance Evaluation of Anti-lock Braking System. *Journal of Engineering Science and Technology*, Volume 14, pp. 30-28.

Digi Technologies CO., LTD, 2000. Digi Technologies CO., LTD. [Online] Available at: http://www.testoshop.vn [Accessed 31 July 2025].

Fu, Q., 2022. Research on Fuzzy Control Method of Automobile Antilock Braking System. *Hindawi*, Volume 2022, pp. 1-9.

Gampa, S.R., Jasthi, K., Alapati, S. and Gudey, S.K. (2023) 'Fuzzy genetic algorithm based antilock braking system', *Proceedings of the International Conference on Artificial Intelligence Techniques for Electrical Engineering Systems*, pp.13–22.

Han, K., Lee, B. & Choi, S. B., 2019. Development of an Antilock Brake System for Electric Vehicles Without Wheel Slip and Road Friction Information. *IEEE Transactions on Vehicular Technology*, Volume 68, pp. 5506-5517.

Kamsi Parts, 2020. Kamsi. [Online] Available at: https://www.kamsiparts.com [Accessed 1 12 2023].

PÁGINA, B. A. E. L., 2019. mecánica Automotriz. [Online] Available at: https://www.ingenieriaynicaautomotriz.com/author/admin/ [Accessed 12 2023].

Phadke, S. B., Shendge, P. D. & Wanaskar, V. S., 2020. Control of antilock braking systems using disturbance observer with a novel nonlinear sliding surface. IEEE Transactions on Industrial Electronics, Volume. 67, no. 8, pp. 6815-6823.

Pretagostini, F. et al., 2020. Survey on Wheel Slip Control Design Strategies Evaluation and Application to Antilock Braking Systems. *IEEE Access*, Volume 8, pp. 10951-10970.

Qi, G., Fan, X., Zhu, S., Chen, X., Wang, P. and Li, H. (2022) 'Research on robust control of automobile anti-lock braking system based on road recognition', *Jordan Journal of Mechanical and Industrial Engineering*, Vol. 16, No. 3, pp.343–352.

Rajguru, S. N., Shah, P., Rayavarapu, N. & Tupe, P., 2014. Application of fuzzy controllers for flow control processes in chemical industries. *Journal of Chemical and Pharmaceutical Research,* Volume 12, pp. 403-410.

Saibabu, V. & Prakash, G. V., 2018. Design and Structural Analysis of Master Cylinder for Pressure Loads. *International Journal of Innovative Technologies,* Volume 6, pp. 0292-0296.

Unguritu, M.-G. & Nichitelea, T.-C., 2023. Design and Assessment of an Anti-lock Braking System Controller. *Romanian Journal of Information Science and Technology*, Volume 26, pp. 21-32.

Vehicle Speed Sensor Kit, n.d. Busaru. [Online] Available at: https://www.busaru.com/busaruparts/speedsensor [Accessed 3 August 2025].

Wang, H., Wu, S. & Qianyu, W., 2021. Global Sliding Mode Control for Nonlinear Vehicle Antilock Braking System. *IEEE Access*, Volume 9, pp. 40349-40359.

Wang, X., Chen, G., Tong, W., Guo, D., Kang, J. and Ren, C. (2022) 'Hardware-in-the-loop simulation of vehicle antilock braking system', *International Journal of Mechatronics and Applied Mechanics*, Vol. 118, No. 12, pp.118–125.

Webdev, 2018. Michigan Scientific Corporation. [Online] Available at: https://www.michsci.com/wheel-speed-sensor-instrumentation/ [Accessed 4 August 2025].

Zhao, C., Ding, H., Cao, G. & Hou, H., 2021. Research on automatic detection technology for the compensation hole shape and position parameters of a brake master cylinder. *Advances in Mechanical Engineering,* Volume 13, pp. 1-16